



UNIVERSITY
OF WOLLONGONG
AUSTRALIA

University of Wollongong
Research Online

Faculty of Science, Medicine and Health - Papers

Faculty of Science, Medicine and Health

2013

Synthesis, structural characterisation, and preliminary evaluation of non-indolin-2-one-based angiogenesis inhibitors related to sunitinib (Sutent[®])

Pichit Sudta
Srinakharinwirot University

Nicholas Kirk
University of Wollongong, nsk597@uowmail.edu.au

Anna Bezos
Australian National University

Anthony Gurlica
University of Wollongong, ag628@uowmail.edu.au

Rhys Mitchell
University of Wollongong, rtm442@uowmail.edu.au

See next page for additional authors

Publication Details

Sudta, P., Kirk, N., Bezos, A., Gurlica, A., Mitchell, R., Weber, T., Willis, A. C., Prabpai, S., Kongsaree, P., Parish, C. R., Suksamrarn, S. & Kelso, M. J. (2013). Synthesis, structural characterisation, and preliminary evaluation of non-indolin-2-one-based angiogenesis inhibitors related to sunitinib (Sutent[®]). *Australian Journal of Chemistry: an international journal for chemical science*, 66 (8), 864-873.

Research Online is the open access institutional repository for the University of Wollongong. For further information contact the UOW Library: research-pubs@uow.edu.au

Synthesis, structural characterisation, and preliminary evaluation of non-indolin-2-one-based angiogenesis inhibitors related to sunitinib (Sutent®)

Abstract

The indolin-2-one fused-ring system and the 2,4-dimethylpyrrole unit represent key structural motifs in the anticancer drug sunitinib (Sutent®) and predecessor angiogenesis inhibitors that have undergone anticancer clinical trials (e.g. semaxinib, SU5416). In pursuit of novel anti-angiogenic scaffolds, we were interested in identifying whether the indolin-2-one group in these structures could be modified without losing activity. This paper describes novel condensation chemistry used to prepare a test series of (E)- and (Z)-alkenes related to SU5416 that retain the 2,4-dimethylpyrrole unit while incorporating ring-opened indolin-2-ones. Unique structural characteristics were identified in the compounds, such as intramolecular hydrogen bonds in the (Z)-alkenes, and several examples were shown to possess significant anti-angiogenic activity in a rat aorta in vitro model of angiogenesis. The work demonstrates that the indolin-2-one moiety is not an absolute requirement for angiogenesis inhibition in the sunitinib/SU5416 class.

Keywords

Angiogenesis inhibitor, SU5416, semaxinib, SU11248, sunitinib, Sutent, indolin-2-one, Knoevenagel, cancer

Disciplines

Medicine and Health Sciences | Social and Behavioral Sciences

Publication Details

Sudta, P., Kirk, N., Bezos, A., Gurlica, A., Mitchell, R., Weber, T., Willis, A. C., Prabpai, S., Kongsaree, P., Parish, C. R., Suksamrarn, S. & Kelso, M. J. (2013). Synthesis, structural characterisation, and preliminary evaluation of non-indolin-2-one-based angiogenesis inhibitors related to sunitinib (Sutent®). *Australian Journal of Chemistry: an international journal for chemical science*, 66 (8), 864-873.

Authors

Pichit Sudta, Nicholas Kirk, Anna Bezos, Anthony Gurlica, Rhys Mitchell, Thomas Weber, Anthony C. Willis, Samran Prabpai, Palangpon Kongsaree, Christopher R. Parish, Sunit Suksamrarn, and Michael J. Kelso

**Synthesis, Structural Characterisation and Preliminary Evaluation of Non-Indolin-2-one-Based
Angiogenesis Inhibitors Related to Sunitinib (Sutent®)**

Pichit Sudta,^{†a} Nicholas Kirk,^{‡a} Anna Bezos,[§] Anthony Gurlica,[‡] Rhys Mitchell,[‡] Thomas Weber,[‡]
Anthony C. Willis,[¥] Samran Prabpai,[£] Palangpon Kongsaree,[£] Christopher R. Parish,[§] Sunit
Suksamrarn,[†] Michael J. Kelso^{‡*}

[†]*Department of Chemistry, Faculty of Science, Srinakharinwirot University, Bangkok (Thailand),*

[‡]*School of Chemistry, Faculty of Science, University of Wollongong, Wollongong, NSW (Australia),*

[§]*Cancer and Vascular Biology Group, Department of Immunology, John Curtin School of Medical
Research, Australian National University, Canberra, ACT (Australia),* [¥]*Single Crystal X-ray*

Diffraction Unit, Research School of Chemistry, Australian National University, Canberra, ACT

(Australia), [£]*Centre for Excellence in Protein Structure and Function, Faculty of Science, Mahidol
University, Bangkok (Thailand).*

^aAuthors contributed equally to this work.

*To whom correspondence should be addressed. Phone: +61 2 4221 5085. Fax: +61 2 4221 4287. E-mail: mkelso@uow.edu.au

Keywords: angiogenesis inhibitor; SU5416; semaxinib; SU11248; sunitinib; Sutent; indolin-2-one; Knoevenagel; cancer

Abbreviations: CSF-1R, colony-stimulating factor-1 receptor; FCS, foetal calf serum; FLT-3, Fms-like tyrosine kinase 3; FOV, field of view; HBSS, Hank's buffered salt solution; Kit, stem cell factor receptor; PDGF[R], platelet-derived growth factor [receptor]; RTKI, receptor tyrosine kinase inhibitors; VEGF[R], vascular endothelial growth factor [receptor].

Abstract

The indolin-2-one fused-ring system and the 2,4-dimethylpyrrole unit represent key structural motifs in the anti-cancer drug sunitinib (Sutent®) and predecessor angiogenesis inhibitors that have undergone anti-cancer clinical trials (e.g. Semaxanib, SU5416). In pursuit of novel anti-angiogenic scaffolds we were interested in identifying whether the indolin-2-one group in these structures could be modified without abrogating activity. This paper describes novel condensation chemistry used to prepare a test series of (*E*) and (*Z*)-alkenes related to SU5416 that retain the 2,4-dimethylpyrrole unit while incorporating ring-opened indoline-2-ones. Unique structural characteristics were identified in the compounds, such as intramolecular hydrogen bonds in the (*Z*)-alkenes, and several examples were shown to possess significant anti-angiogenic activity in a rat aorta *in vitro* model of angiogenesis. The work demonstrates that the indolin-2-one moiety is not an absolute requirement for angiogenesis inhibition in the sunitinib/SU5416 class.

1. Introduction

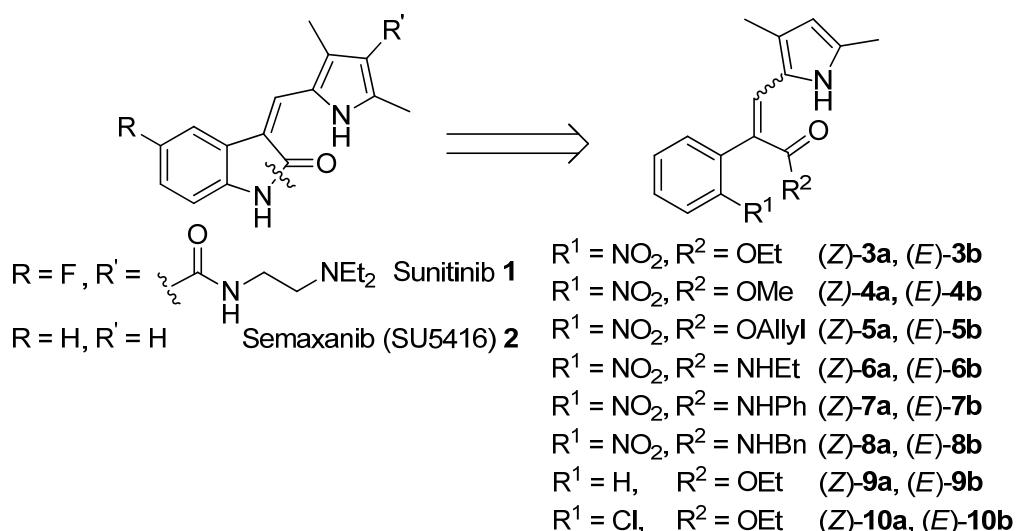
Angiogenesis, the growth of new blood vessels from pre-existing vascular networks, occurs only under certain conditions in adults such as during wound healing, pregnancy and menstruation, but can be much more prevalent in pathological conditions, especially cancer.^[1,2] Solid tumours which grow beyond 1~2 mm require angiogenesis to avoid becoming hypoxic from the effects of growth factor mutation-induced aberrant blood vessel formation and increased energy consumption.^[3] In the absence of angiogenesis, solid tumours enter latent phases and rely on anaerobic metabolism for energy limiting their growth.^[2,3] Angiogenesis is also a major contributor to metastasis as the newly formed vessels provide a route for tumour cells to enter the circulation.^[3] Accordingly, inhibitors of angiogenesis have been intensely studied as anti-cancer agents and several have been approved for clinical use.^[4]

The first FDA-approved angiogenesis inhibitor was the vascular endothelial growth factor (VEGF)-targeting monoclonal antibody (Mab) Bevacizumab (Avastin®; Genentech Inc., 2003), which continues to be used today in combination therapies against metastatic colorectal cancer,^[5] non-small cell lung cancer^[6] and metastatic breast cancer.^[7] Newer VEGF-targeting agents are in various stages of clinical development, including, for example, VEGF-Trap_{R1R2} (Aflibercept; Regeneron Inc.), a chimeric soluble VEGF receptor that binds to and neutralises VEGF.^[8] In addition to these biologics, small molecule receptor tyrosine kinase inhibitors (RTKIs) targeting VEGF receptors (VEGFR1–VEGFR3) and other kinase signalling pathways have been extensively investigated as anti-angiogenics and several have progressed to the market. These include sunitinib **1** (Sutent®; Pfizer),^[9] pazopanib (Votrient®, GSK),^[10] sorafenib (Nexavar®; Bayer)^[11] and vandetanib (Caprelsa®, AstraZeneca).^[12]

Sunitinib **1** (Figure 1) is approved for the treatment of highly vascularised renal cell carcinomas,^[13]

gastrointestinal stromal tumours^[14] and pancreatic neuroendocrine tumours.^[15] Its mechanism of action involves inhibition of at least eight different receptor tyrosine kinases, including VEGF1-VEGF3, platelet-derived growth factor receptors (PDGFR α and PDGFR β), stem cell factor receptor (Kit), FLT-3 and colony-stimulating factor-1 receptor (CSF-1R).^[16] During development the indolin-2-one (oxindole) and 2,4-dimethylpyrrole portions of Sunitinib **1** were identified as key pharmacophores and were retained throughout med-chem optimisation efforts. Several other closely related compounds which contain these groups were also (and continue to be) evaluated in clinical trials.^[17] For example, the structurally simpler sunitinib predecessor semaxanib (SU5416) **2** (Figure 1) underwent a Phase III clinical trial for advanced colorectal cancer.

Figure 1. Structures of sunitinib **1**, semaxanib (SU5416) **2** and alkenes (*Z*)-**3a**, (*E*)-**3b** – (*Z*)-**10a**, (*E*)-**10b**.



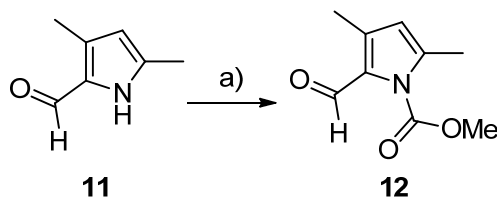
In pursuit of novel and patentable anti-angiogenic scaffolds, we hypothesised that in spite of its perceived importance the indolin-2-one moiety may not be essential for anti-angiogenic activity in the sunitinib/SU5416 class. The hypothesis has been explored in the current work using a test series of SU5416-like alkenes that attach the 2,4-dimethylpyrrole unit to ring-opened indoline-2-ones (i.e.

compounds (*Z*)-**3a**, (*E*)-**3b** – (*Z*)-**10a**, (*E*)-**10b**, Figure 1). This paper details the synthesis of the series using novel condensation chemistry, describes some of the unique structural characteristics of the alkenes, as identified by NMR spectroscopy and x-ray crystallography, and reports that several members show significant anti-angiogenic activity in a rat aorta *in vitro* model of angiogenesis.

2. Chemistry

Initial synthetic efforts aimed to identify a general condensation reaction that could provide access to the target alkenes. In the reported syntheses of sunitinib **1**, SU5416 **2** and related indolin-2-ones, the base indoline-2-ones and requisite *N*-unsubstituted pyrrole-2-carboxaldehydes were condensed by refluxing the two components in ethanol with piperidine.^[18] Attempts to adapt this procedure to the condensation of the model substrate ethyl-2-(2-nitrophenyl)-acetate **13** and 3,5-dimethylpyrrole-2-carboxaldehyde **11** failed to yield any of the desired alkenes (*Z*)-**3a** or (*E*)-**3b**). Other Knoevenagel or Perkin-type condensations attempted with **13** and **11** using various bases and solvents and under a variety of conditions were similarly unsuccessful. At this point it was reasoned that the aldehyde in **11** was unreactive due to a combination of steric hindrance from the neighbouring pyrrole 3-Me group and because electron donation from the pyrrole nitrogen into the aldehyde was reducing its electrophilic character. It was postulated that a small electron withdrawing group attached to the pyrrole nitrogen should increase the aldehyde's reactivity without increasing steric hinderance. Attaching electron withdrawing groups to pyrrole nitrogens has previously been shown to activate aldehydes at the 2-position.^[19,20] Accordingly, *N*-methylcarbamoyl pyrrole-2-carboxaldehyde **12** was prepared in 86% yield by acylating the potassium salt of **11** (formed by *N*-deprotonation of **11** with KH in THF at 0 °C) with methyl chloroformate (Scheme 1).

Scheme 1. Synthesis of *N*-methylcarbamoyl pyrrole aldehyde **12**.^a

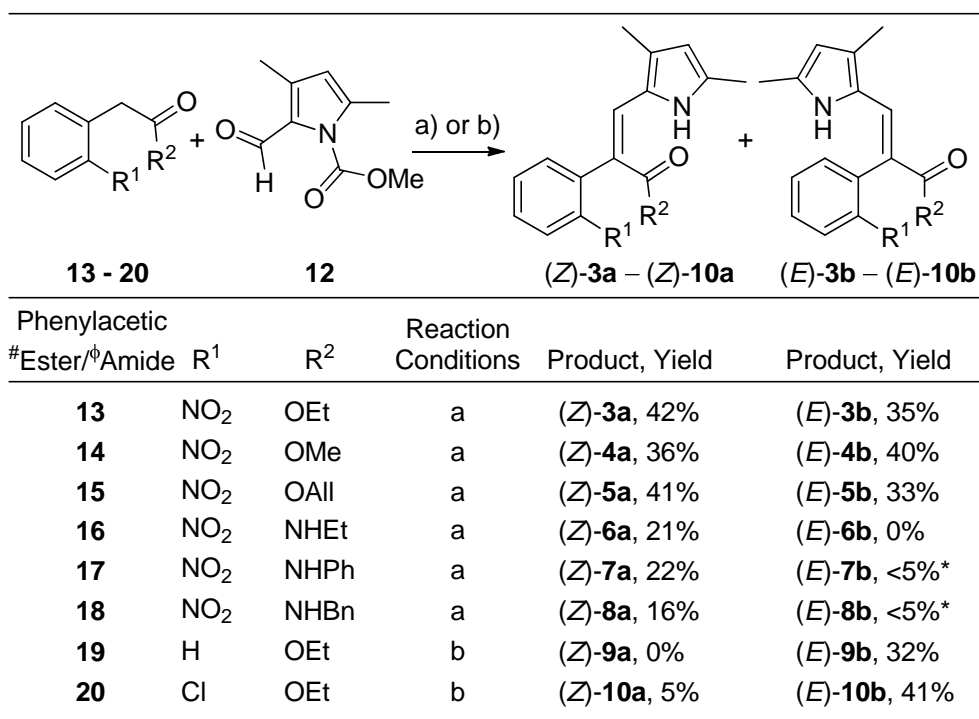


^aReagents and conditions: (a) (i) KH, THF, 0 °C, (ii) CH₃OC(=O)Cl, 2 h, (86%).

Stirring ethyl-2-(2-nitrophenyl)-acetate **13** with **12** in refluxing THF in the presence of K₂CO₃ and 18-crown-6 (Method a, Figure 2) was found to directly afford the pyrrole *N*-deprotected Knoevenagel condensation products (*Z*)-**3a** (42%) and (*E*)-**3b** (35%). Similar yields of the desired *N*-deprotected (*Z*) and (*E*)-alkenes were obtained directly from reactions of **12** with methyl-2-(2-nitrophenyl)-acetate **14** and allyl-2-(2-nitrophenyl)-acetate **15** (i.e. (*Z*)-**4a**, (*E*)-**4b** and (*Z*)-**5a**, (*E*)-**5b**, respectively). The condensation reactions did not proceed when the *N*-methyl carbamoyl group of **12** was replaced with either *N*-ethyl or *N*-^tButyl carbamates, possibly due to increased steric hindrance around the aldehyde.

Use of *N*-alkyl- or *N*-aryl-2-(2-nitrophenyl)-acetamides in place of 2-(2-nitrophenyl)-acetic esters led to reduced yields of the *Z*-isomers and none or very low yields of the *E*-isomers. Nevertheless, several amides were able to be isolated in sufficient quantity and purity (> 95% by ¹H NMR) for characterisation and angiogenesis inhibition testing. Use of *N*-Ethyl-2-(2-nitrophenyl)-acetamide **16** in the reaction afforded a 21% yield of (*Z*)-**6a** without formation of any (*E*)-**6b**. *N*-Phenyl-2-(2-nitrophenyl)-acetamide **17** and *N*-benzyl-2-(2-nitrophenyl)-acetamide **18** yielded 22% and 16% yields, respectively, of alkenes (*Z*)-**7a** and (*Z*)-**8a**, with less than 5% of the *trans*-isomers (*E*)-**7b** and (*E*)-**8b** being isolated. All alkenes except (*E*)-**7b** and (*E*)-**8b** were tested for angiogenesis inhibition.

Figure 2. Synthesis of alkenes (*Z*)-**3a**, (*E*)-**3b** – (*Z*)-**10a**, (*E*)-**10b**.^a



*Compounds could not be isolated in pure form. [#]Esters **13–15,19,20** were synthesised by refluxing the phenylacetic acids in the requisite alcohol (as solvent) with H₂SO₄ (cat.).

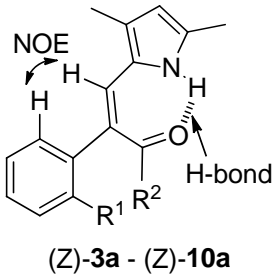
^φAmides **16–18** were obtained by stirring 2-nitro-phenylacetic acid with the requisite amines under standard solution phase peptide coupling conditions (i.e. HBTU/DIPEA in CH₂Cl₂).

^aReagents and conditions: (a) K₂CO₃, 18-crown-6, THF, reflux, 16 h; (b) LDA, THF, -78 °C, 30 min.

In our structure-activity study it was of interest to establish the importance of the 2-nitro group for angiogenesis inhibition. Alkenes (*Z*)-**9a**, (*E*)-**9b**, (*Z*)-**10a** and (*E*)-**10b** were targeted for this purpose. However, attempts to perform the condensation (Figure 2, Method a) with **12** and either ethyl-2-phenylacetate **19** or ethyl-2-(2-chlorophenyl)-acetate **20** were unsuccessful, thus highlighting the requirement for the *ortho*-nitro group in this reaction. Switching to the stronger base LDA and carrying the reaction out with ethyl-2-phenylacetate **19** in THF at -78 °C (Figure 2, Method b) afforded a 32%

yield of the *trans* alkene (*E*)-**9b** while none of the *cis* alkene (*Z*)-**9a** was formed. Applying the same procedure with 2-(2-chlorophenyl)-acetate **20** yielded 41% of (*E*)-**10b** and 5% of the *cis* isomer (*Z*)-**10a**.

Figure 3. (a) *cis*-stereochemistry was confirmed in (*Z*)-**3a** – (*Z*)-**10a** by the presence of an NOE between the vinylic proton and *ortho* proton on their respective phenyl rings. (b) Comparison of the pyrrole NH chemical shift values in the ¹H NMR spectra of *cis*-alkenes (*Z*)-**3a** – (*Z*)-**10a** and *trans*-alkenes (*E*)-**3b** – (*E*)-**10b**. The downfield-shifted signals in the *cis*-series are indicative of intramolecular hydrogen bonds between the pyrrole NH and carbonyl oxygen atoms.

(a) 
(Z)-**3a** - (*Z*)-**10a**

(b)

<i>cis</i> -alkenes		<i>trans</i> -alkenes	
Compound	Pyrrole NH chemical shift (ppm)	Compound	Pyrrole NH chemical shift (ppm)
(<i>Z</i>)- 3a	11.89	(<i>E</i>)- 3b	6.80
(<i>Z</i>)- 4a	11.82	(<i>E</i>)- 4b	6.74
(<i>Z</i>)- 5a	12.91	(<i>E</i>)- 5b	6.75
(<i>Z</i>)- 6a	12.21	(<i>E</i>)- 6b	N/A
(<i>Z</i>)- 7a	12.00	(<i>E</i>)- 7b	6.47
(<i>Z</i>)- 8a	12.21	(<i>E</i>)- 8b	N/A
(<i>Z</i>)- 9a	N/A	(<i>E</i>)- 9b	6.84
(<i>Z</i>)- 10a	11.80	(<i>E</i>)- 10b	6.75

N/A not available

Cis-stereochemistry was confirmed in alkenes (*Z*)-**3a** – (*Z*)-**10a** from 2D-NOESY spectra which in all cases showed NOE cross-peaks between the vinylic proton and the *ortho* proton on the phenyl ring (Figure 3a). A second feature common to all *cis*-isomers was a downfield chemical shift of the pyrrole NH signals (11.80 – 12.91 ppm) in their ¹H NMR spectra relative to the corresponding *trans*-isomers (6.47 – 6.87 ppm, Figure 3b). These strongly deshielded signals suggested the presence of intramolecular hydrogen bonds in the *cis*-alkenes between the pyrrole NH and carbonyl oxygen

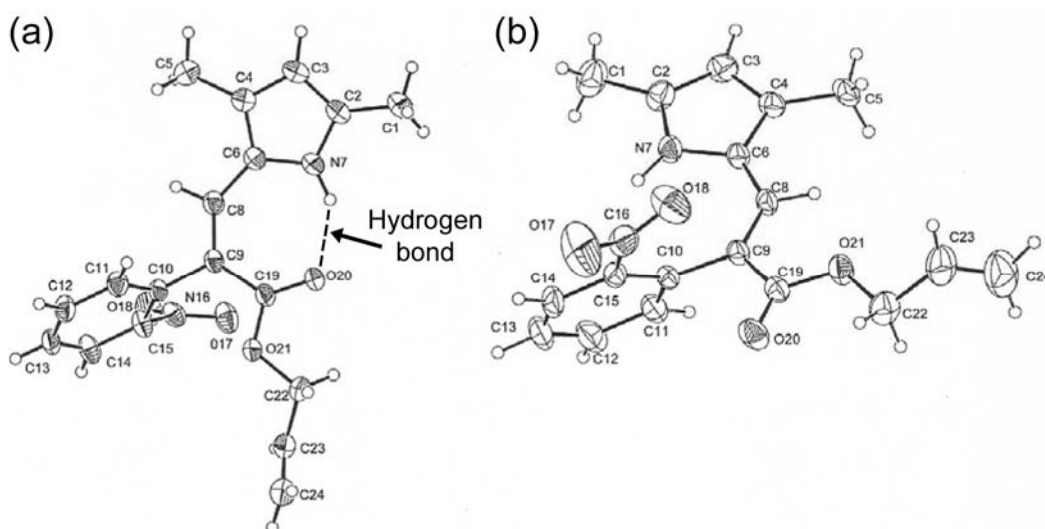
atoms.^[21] Furthermore, the *cis*-isomers were all observed to be significantly less polar than their corresponding *trans*-isomers (by TLC) which, in addition to simplifying purification by silica-gel column chromatography, supported the presence of the hydrogen bonds. The presence of an intramolecular hydrogen bond in allyl ester (*Z*)-**5a** was eventually confirmed (in the solid state) by x-ray crystallography (Figure 4a). It is noteworthy that analogous hydrogen bonds are found in SU5416 **2** and related indolin-2-one-based angiogenesis inhibitors which contain (*Z*)-alkenes.^[22]

The ¹H NMR spectrum of (*E*)-**3b** displayed an unusual pair of doublet-of-quartet signals at 4.10 ppm and 4.23 ppm (total integration 2H) suggesting the presence of diastereotopic ethyl ester CH₂ protons (Supplementary Data, Figure S1 (b)). In contrast, the CH₂ group of (*Z*)-**3a** displayed the expected first-order quartet at 4.12 ppm. (Supplementary Data, Figure S1 (a)). Complex methylene signals were similarly observed for the allyl ester methylene CH₂ of (*E*)-**5b** (2 x doublet-of-doublets at 4.59 ppm and 4.64 ppm) and the ethyl ester CH₂ group of (*E*)-**10b** (2 x quartets at 4.18 ppm and 4.25 ppm). Such observations are consistent with the di-substituted phenyl rings of these compounds being unable to freely rotate about the *ipso* Ar-C bond due to a steric clash between the bulky *ortho*-phenyl ring substituents (i.e. *ortho*-NO₂ in (*E*)-**3b** and (*E*)-**5b** and *ortho*-Cl in (*E*)-**10b**) and the pyrrole ring located on the same side of the alkene double bond (Supplementary Data, Figure S1 (c)). The restricted rotation and resulting axial double-bond chirality in these “overcrowded” alkenes explains the presence of diastereotopic CH₂ signals in the ¹H NMR spectra. That the CH₂ group of (*E*)-**9b** (which contains no aryl *ortho*-substituent) produced a simple quartet at 4.22 ppm supports this explanation, as does the appearance of the CH₂ groups of *cis*-alkenes (*Z*)-**5a**, (*Z*)-**6a** and (*Z*)-**10a** as first-order quartets (integration 2H), and the benzyl CH₂ group of (*Z*)-**8a** as a simple doublet (integration 2H).

Single crystal x-ray structures were obtained for the pair of allyl esters (*Z*)-**5a** and (*E*)-**5b** (Figure 4). The solid-state structure of (*Z*)-**5a** provided clear evidence for an intramolecular hydrogen bond

stabilising a pseudo-7-membered ring within its structure. The inter-atomic distance between the pyrrole nitrogen and the carbonyl oxygen atom in the crystal structure was very short (2.7 Å) suggesting that the hydrogen bond in (*Z*)-**5a** is relatively strong.^[21] The x-ray structure of (*E*)-**5b** showed no intramolecular hydrogen bonds.

Figure 4. ORTEP plots of allyl esters (a) (*Z*)-**5a** and (b) (*E*)-**5b**. An intramolecular hydrogen bond was observed in (*Z*)-**5a** between the pyrrole N-H and carbonyl oxygen atoms (N7 to O20 distance = 2.7 Å).



3. Angiogenesis Inhibition

The alkenes were tested for anti-angiogenic effects using our previously reported rat aorta *in vitro* model of angiogenesis (Figure 5).^[23] In this assay, thoracic aortic sections are excised from female Fischer 344 rats and suspended in a fibrin gel matrix in 48-well plates. A minimum of six replicate cultures for each compound treatment (at each concentration) are prepared. The cultures are fed on Day 4 and vessel outgrowths from the rings measured on Day 5. Angiogenesis is visualised under a microscope (40 x magnification) and quantified manually as the percentage of the field of view (FOV) around the vessel fragment occupied by new vessel outgrowths (i.e. FOV %). Under these conditions, absence of test compound produces 85.7% FOV occupancy (Figure 5; Control: no compound).

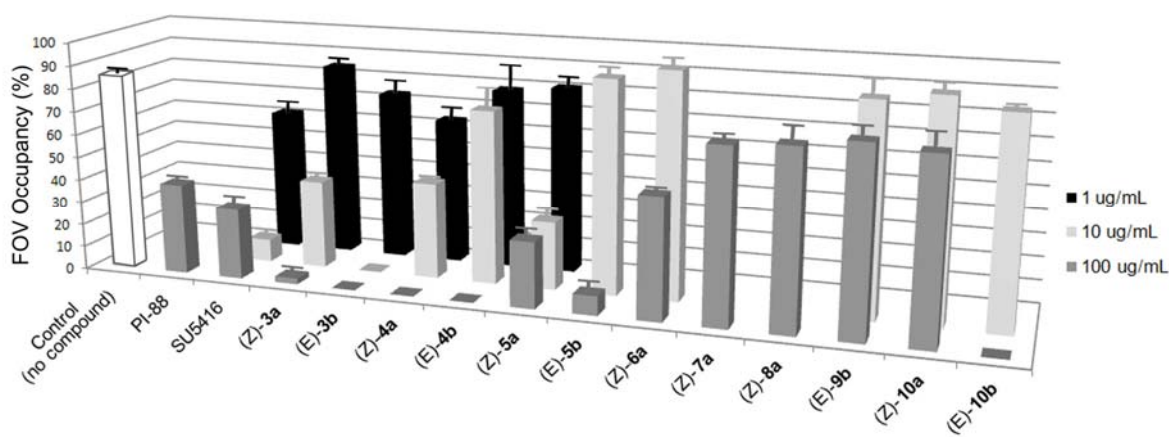
Two positive controls PI-88 and SU5416 **2** were included in the assays. PI-88 is a highly sulfated oligosaccharide-based angiogenesis inhibitor^[24] currently undergoing Phase III clinical trials as a single treatment following cancer surgery in subjects with hepatitis virus-related hepatocellular carcinoma.^[25] At 100 µg/mL, PI-88 reduced FOV occupancy to 39.2%. SU5416 **2** produced an unusual response where greater inhibition of angiogenesis was observed at 10 µg/mL (FOV occupancy 9.7%) than at 100 µg/mL (FOV occupancy 30.6%), while 61.4% FOV occupancy was observed at 1 µg/mL. Small crystals observed in wells containing 100 µg/mL SU5416 **2** suggested that its low solubility in the medium may have caused the poor dose dependency.

Ethyl and methyl esters (*Z*)-**3a**, (*E*)-**3b**, (*Z*)-**4a** and (*E*)-**4b** were found to completely inhibit angiogenesis at 100 µg/mL. At 10 µg/mL (*E*)-**3b** continued to show complete inhibition whereas the other three esters all showed significantly diminished effects at this concentration. At 1 µg/mL, the four esters showed either minimal effects (< 20% difference relative to negative control) or no activity. Surprisingly, the *cis*-allyl ester (*Z*)-**5a** showed the same level of inhibition at both 100 µg/mL and 10 µg/mL (FOV occupancy 28.3% and 29.3%, respectively) but no activity at 1 µg/mL. For the *trans*-allyl ester (*E*)-**5b**, strong activity was observed at 100 µg/mL (FOV occupancy 8.3%) but this activity was completely abolished at 10 µg/mL. We conclude from the data that (*E*)-**3b** is the most active of the 2-nitrophenylacetic ester series.

The *cis*-ethylamide (*Z*)-**6a** showed reduced effects (FOV occupancy 51.7% at 100 µg/mL, inactive at 10 µg/mL) relative to (*Z*)-**3a**, indicating that directly substituting the ester group for an amide is detrimental for activity. Observing that amides (*Z*)-**7a** and (*Z*)-**8a** were inactive at 100 µg/mL supported this conclusion. Removal of the NO₂ group from the phenyl ring was found to completely abolish

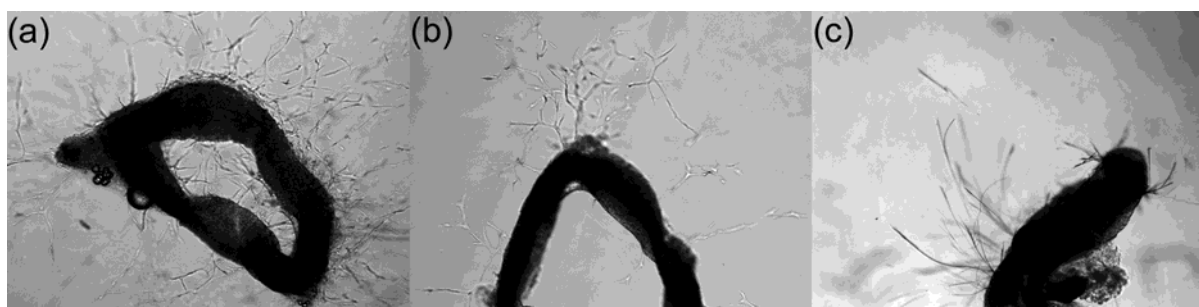
activity (i.e. (*E*)-**9b** vs (*E*)-**3b**). Interestingly, replacing the NO₂ group with Cl had no effect on activity at 100 µg/mL, with both (*E*)-**10b** and (*E*)-**3b** completely inhibiting angiogenesis, but at 10 µg/mL (*E*)-**10b** showed no activity.

Figure 5. Inhibition of angiogenesis by alkenes (*Z*)-**3a**, (*E*)-**3b** – (*Z*)-**10a**, (*E*)-**10b** relative to negative control (no compound) and positive controls PI-88^[24] (100 µg/mL) and SU5416 **2**. Female Fischer 344 rat thoracic aortic sections were cultured in a gel fibrin matrix in 48-well plates in the presence/absence of compounds. Cultures were fed on Day 4 and vessel outgrowths measured on Day 5.^[23] Wells were visualised under 40 x magnification and the percentage of the field of view (FOV) occupied by vessel outgrowths reported as FOV occupancy (%). Negative control (no compound, unshaded bar) showed 85.7 % FOV occupancy. Compounds showing little or no activity at higher concentrations were not tested at lower concentration(s). Data represent the mean FOV occupancy (%) generated from at least six replicate cultures of each test compound at each concentration tested. (See Supplementary Data Table S1 for statistics).



Visual inspection of the assay wells on Day 5 revealed that outgrowths sprouting from rings cultured in the presence of SU5416 **2** (100 $\mu\text{g}/\text{mL}$) differed markedly in morphology from those sprouting from control rings (no compound) or from rings cultured in the presence of PI-88 (100 $\mu\text{g}/\text{mL}$) or alkenes (e.g. (*Z*)-**3a**, 100 $\mu\text{g}/\text{mL}$) (Figure 6). While the outgrowths from the control rings and rings grown in the presence of PI-88 or alkenes showed normal morphology, outgrowths from the SU5416 **2** treated rings consisted of fine hair-like structures which lacked a visible lumen. At lower concentrations of SU5416 **2** (10 $\mu\text{g}/\text{mL}$) the outgrowths showed normal morphology.

Figure 6. Morphology of vessel outgrowths from rat aortic rings cultured in the presence of: (a) Control (no compound), (b) PI-88 (100 $\mu\text{g}/\text{mL}$) and (c) SU5416 **2** (100 $\mu\text{g}/\text{mL}$). The outgrowths from control rings and rings grown in the presence of PI-88 (and (*Z*)-**3a**; image not shown) appeared normal whereas rings cultured in the presence SU5416 **2** produced fine hair-like outgrowths with no lumen.



4. Concluding Remarks

In summary, a novel series of alkenes (*Z*)-**3a**, (*E*)-**3b** – (*Z*)-**10a**, (*E*)-**10b** was synthesised to test the hypothesis that anti-angiogenic activity can be retained in structures related to semaxanib (SU5416) **2**, a structurally simpler predecessor of the FDA approved drug sunitinib, when the indolin-2-one moiety is modified through ring opening. The 2,4-dimethylpyrrole portion of SU5416 **2** was retained in the test compounds to strengthen conclusions regarding the importance of the indoline-2-one group. *In vitro* angiogenesis inhibition assays revealed that several of the alkene esters, including both (*Z*) and (*E*)-

isomers, showed significant anti-angiogenic effects. Compound (*E*)-**3b** emerged as the most potent showing complete inhibition of angiogenesis at 10 µg/mL. The work provides evidence that the indolin-2-one moiety is not essential for anti-angiogenic activity in the sunitinib/SU5416-type class.

The novel condensation chemistry developed to access the target series has scope for wider explorations. For example, while the *ortho*-NO₂ group was found to be necessary for successful reactions with phenylacetic esters and amides it would be of interest to explore whether this group can be moved to the *meta* or *para* positions on the phenyl ring and whether it can be replaced altogether with other electron withdrawing groups. Additionally, it is likely that **12** could be useful as a 3,5-dimethylpyrrole-2-carboxaldehyde surrogate in condensation reactions with carbanions derived from substrates other than phenylacetic esters and amides. It is also tempting to speculate that pyrrole *N*-methyl carbamoylation might be a more generally useful tactic in condensation reactions with other pyrrole-2-carboxaldehydes where either enhanced aldehyde reactivity and/or pyrrole *N*-protection is required.

5. Experimental Section

5.1. Chemistry.

3,5-Dimethylpyrrole-2-carboxaldehyde **11** was purchased from Sigma-Aldrich. Semaxanib (SU5416) **2** was synthesised in-house using a novel (unpublished) procedure. The spectroscopic data for the synthesised Semaxanib was identical in all respects to that reported in the literature.^[22] Anhydrous tetrahydrofuran (THF) was freshly distilled from sodium benzophenone ketyl. Anhydrous CH₂Cl₂ was freshly distilled from CaH₂. All other solvents were of analytical reagent (AR) grade and used without further purification. The term petroleum spirit refers to petroleum spirit within the boiling range 40 – 60 °C. Column chromatography was performed using silica gel 60 (230–400 mesh, Merck). Reaction monitoring by thin layer chromatography (TLC) was carried out using Merck Silica Gel 60 F254 (0.2

mm) plates. Compounds were visualized by examination under UV light and/or by staining with cerium ammonium molybdate. ^1H and ^{13}C NMR spectra were recorded on a Varian-Inova-500 MHz spectrometer. Chemical shifts (δ) are expressed in ppm relative to tetramethylsilane (0 ppm). Signal splitting patterns are described as singlet (s), broad singlet (br s), doublet (d), triplet (t), broad triplet (br t), multiplet (m) or a combination of the above. IR spectra were recorded using a Nicolet Avatar 360 FT-IR spectrometer with characteristic absorption bands reported in wavenumbers [cm^{-1}]. High resolution electrospray ionisation mass spectra were recorded using a factory modified Waters QToF *Ultima* Mass Spectrometer (Wynteshawe, UK). Melting points were determined using a Reichert melting point apparatus and are uncorrected.

Methyl 2-formyl-3,5-Dimethyl-1H-pyrrole-1-carboxylate (12): 3,5-dimethylpyrrole-2-carboxaldehyde **11** (1.47 g, 11.9 mmol) in anhydrous THF (10 mL) was added dropwise over 10 min to a stirring suspension of potassium hydride (0.57 g, 14.3 mmol) in dry THF (50 mL) under N_2 at 0 °C. Following complete addition the mixture was allowed to stir at 0 °C for a further 30 minutes. Methyl chloroformate (2.48 g, 26.2 mmol) diluted in anhydrous THF (10 mL) was then added dropwise to the stirring mixture at 0 °C over ten minutes. The reaction was allowed to warm slowly to room temperature and stirred for a further 2 hours while monitoring by TLC analysis (petroleum spirit:acetone, 80:20). After complete consumption of starting material the reaction was quenched with ice-cold H_2O (30 mL) and stirred for 15 min. The crude mixture was extracted with EtOAc (3 x 25 mL) and the combined organic extracts washed with H_2O (25 mL) and brine (25 mL) before drying over anhydrous MgSO_4 and concentrating *in vacuo*. The crude product was purified by silica-gel column chromatography using a gradient from 100:0 to 95:5 petroleum spirit:acetone to provide **12** (1.83 g, 85%) as a white crystalline solid. $R_f = 0.53$ (80:20 petroleum spirit:acetone), m.p. 44-45 °C; ^1H NMR (500 MHz, CDCl_3 ,): δ 2.34 (s, 3H), 2.42 (s, 3H), 4.00 (s, 3H), 5.93 (s, 1H), 10.03 (s, 1H); ^{13}C NMR

(125 MHz, CDCl₃): δ 12.9, 15.2, 54.3, 115.9, 130.3, 135.8, 138.2, 151.5, 181.2; IR (neat): $\nu(\text{cm}^{-1}) = 1730, 1650, 1496, 1451, 1326, 1153, 765 \text{ cm}^{-1}$; HRMS-ESI: m/z [M+H]⁺ calcd for C₉H₁₁NO₃ 182.0812, observed 182.0817.

General method for the synthesis of 2-phenylacetic esters 13-15, 19, 20: A solution of the requisite 2-phenylacetic acid (~ 3 g) in the appropriate alcohol (40 mL) with 5 drops of concentrated sulfuric acid added was stirred at reflux under N₂. Upon complete disappearance of starting material (TLC; petroleum spirit:acetone, 70:30) the reaction mixture was allowed to cool to room temperature before removing the alcohol by evaporation *in vacuo*. The crude residue was diluted with EtOAc (50 mL), added to a separating funnel and washed with saturated aqueous Na₂CO₃ (30 mL), H₂O (3 x 25 mL), and brine (30 mL). The organic layer was then dried over anhydrous MgSO₄ and concentrated *in vacuo*.

Ethyl-2-(2-nitrophenyl)-acetate (13): 97%, white crystalline solid; m.p. 61-63 °C; ¹H NMR (500 MHz, CDCl₃): δ 1.16 (t, 3H, $J = 7.0$ Hz), 3.93 (s, 2H), 4.07 (q, 2H, $J = 7.0$ Hz), 7.28 (d, 1H, $J = 7.5$ Hz), 7.38 (t, 1H, $J = 8.0$ Hz), 7.50 (t, 1H, $J = 7.5$ Hz), 7.99 (d, 1H, $J = 8.0$ Hz); ¹³C NMR (125 MHz, CDCl₃): δ 13.7, 39.4, 60.9, 124.9, 128.2, 129.5, 132.9, 133.2, 148.5, 170.0. HRMS-ESI: m/z [M+H]⁺ calcd for C₁₀H₁₂NO₄ 210.0761, observed 210.0757.

Methyl-2-(2-nitrophenyl)-acetate (14): 97%, pale yellow oil; ¹H NMR (500 MHz, CDCl₃): δ 3.68 (s, 3H), 4.00 (s, 2H), 7.34 (d, 1H, $J = 8.0$ Hz), 7.45 (t, 1H, $J = 8.0$ Hz), 7.57 (t, 1H, $J = 8.0$ Hz), 8.08 (d, 1H, $J = 8.0$ Hz); ¹³C NMR (125 MHz, CDCl₃): δ 39.8, 52.5, 125.5, 128.9, 133.5, 133.6, 133.8, 148.9, 170.6. HRMS-ESI: m/z [M+H]⁺ calcd for C₉H₁₀NO₄ 196.0604, observed 196.0615.

Allyl-2-(2-nitrophenyl)-acetate (15): 88%, pale yellow oil; ^1H NMR (500 MHz, CDCl_3): δ 4.04 (s, 2H), 4.60 (dd, 2H, $J = 1.5, 4.5$ Hz), 5.21 (dd, 1H, $J = 1.5, 10.0$ Hz), 5.28 (dd, 1H, $J = 1.5, 17.0$ Hz), 5.89 (m, 1H), 7.35 (d, 1H, $J = 7.5$ Hz), 7.46 (t, 1H, $J = 7.5$ Hz), 7.58 (t, 1H, $J = 7.5$ Hz), 8.09 (d, 1H, $J = 7.5$ Hz); ^{13}C NMR (125 MHz, CDCl_3): δ 39.8, 66.0, 118.7, 125.4, 128.8, 132.0, 133.6, 133.8, 148.5, 169.8. ESI-MS: 222.3 $[\text{M} + \text{H}]^+$. HRMS-ESI: m/z $[\text{M} + \text{H}]^+$ calcd for $\text{C}_{11}\text{H}_{12}\text{NO}_4$ 222.0761, observed 222.0733.

Ethyl-2-phenylacetate (19): 80%, pale yellow oil; ^1H NMR (500 MHz, CDCl_3): δ 1.23 (t, 3H, $J = 7.0$ Hz), 3.56 (s, 2H), 4.13 (q, 2H, $J = 7.0$ Hz), 7.29 (m, 5H); ^{13}C NMR (125 MHz, CDCl_3): δ 14.2, 41.4, 60.8, 128.0, 134.3, 171.6. HRMS-ESI: m/z $[\text{M} + \text{H}]^+$ calcd for $\text{C}_{10}\text{H}_{13}\text{O}_2$ 165.0910, observed 165.0914.

Ethyl-2-(2-chlorophenyl)-acetate (20): 71%, pale yellow oil; ^1H NMR (500 MHz, CDCl_3): δ 1.20 (t, 3H, $J = 7.0$ Hz), 3.71 (s, 2H), 4.12 (q, 2H, $J = 7.0$ Hz), 7.23 (m, 4H); ^{13}C NMR (125 MHz, CDCl_3): δ 14.0, 38.9, 60.7, 128, 132.4, 134.3, 170.5. HRMS-ESI: m/z $[\text{M} + \text{H}]^+$ calcd for $\text{C}_{10}\text{H}_{12}\text{ClO}_2$ 199.0520, observed 199.0526.

General procedure for the synthesis of *N*-alkyl/aryl-2-(2-nitrophenyl)-acetamides 16-18: A dry round-bottom flask under N_2 was charged with 2-nitrophenylacetic acid (324 mg, 1.79 mmol), amine (2.42 mmol), HBTU (709 mg, 1.87 mmol) and CH_2Cl_2 (10 mL) before adding DIPEA (3.85 mmol). The solution was stirred at room temperature while monitoring by TLC analysis (petroleum spirit:acetone, 80:20). Upon complete consumption of starting material the reaction was diluted with CH_2Cl_2 (30 mL) and washed with 5% HCl (3 x 25 mL), saturated aqueous Na_2CO_3 (3 x 25 mL) and brine (30 mL). The organic layer was dried over anhydrous MgSO_4 and concentrated to afford the pure amide.

N-Ethyl-2-(2-nitrophenyl)-acetamide (16): 57%, white amorphous solid; m.p. 137-139 °C; ¹H NMR (500 MHz, CDCl₃): δ 1.13 (t, 3H, *J* = 7.0 Hz), 3.29 (q, 2H, *J* = 7.0 Hz), 3.81 (s, 2H), 5.80 (br s, 1H), 7.45 (t, 1H, *J* = 7.5 Hz), 7.50 (d, 1H, *J* = 7.5 Hz), 7.60 (t, 1H, *J* = 7.5 Hz), 8.02 (d, 1H, *J* = 8.5 Hz); ¹³C NMR (125 MHz, CDCl₃): δ 15.0, 35.0, 41.1, 125.3, 128.6, 130.7, 133.6, 133.8, 149.1, 169.0. HRMS-ESI: *m/z* [M+H]⁺ calcd for C₁₀H₁₃N₂O₃ 209.0921, observed 209.0924.

N-Phenyl-2-(2-nitrophenyl)-acetamide (17): 95%, off-white amorphous solid; m.p. 141-143 °C; ¹H NMR (500 MHz, CDCl₃): δ 4.03 (s, 2H), 7.08 (t, 1H, *J* = 7.5 Hz), 7.28 (t, 2H, *J* = 7.5 Hz), 7.47 (m, 3H), 7.54 (d, 1H, *J* = 7.0 Hz), 7.61 (t, 1H, *J* = 7.5 Hz), 7.82 (br s, 1H), 8.05 (d, *J* = 8.5 Hz); ¹³C NMR (125 MHz, CDCl₃): δ 41.9, 119.9, 124.4, 125.2, 128.6, 128.9, 130.0, 133.4, 133.7, 167.2. HRMS-ESI: *m/z* [M+H]⁺ calcd for C₁₄H₁₃N₂O₃ 257.0921, observed 257.0929.

N-Benzyl-2-(2-nitrophenyl)-acetamide (18): 95%, off-white amorphous solid; m.p. 136-138 °C; ¹H NMR (500 MHz, CDCl₃): δ 3.88 (s, 2H), 4.45 (d, 2H, *J* = 6 Hz), 6.12 (br s, 1H), 7.26 (t, 3H, *J* = 8.0 Hz), 7.31 (t, 2H, *J* = 7.5 Hz), 7.45 (t, 1H, *J* = 7.5 Hz), 7.51 (d, 1H, *J* = 7.5 Hz), 7.60 (t, 1H, *J* = 7.5 Hz), 8.04 (d, 1H, *J* = 8.5 Hz); ¹³C NMR (125 MHz, CDCl₃): δ 40.9, 43.8, 125.1, 127.5, 127.6, 128.5, 128.7, 130.2, 133.5, 133.6, 137.9, 148.9, 169.0. HRMS-ESI: *m/z* [M+H]⁺ calcd for C₁₅H₁₅N₂O₃ 271.1077, observed 271.1065.

General method for condensation reactions to produce alkenes (Z)-3a, (E)-3b – (Z)-8a, (E)-8b:

Method a: To a dry round bottom flask under N₂ was added anhydrous potassium carbonate (1.205 g, 8.73 mmol) in dry THF (15 mL) followed by 18-crown-6 (0.575 g, 2.18 mmol). The mixture was stirred at room temperature for 10 minutes before adding a solution of the appropriate 2-(2-

nitrophenyl)-acetate/acetamide (4.36 mmol) in dry THF (10 mL) and heating at reflux for 3 hours. Methyl 2-formyl-3,5-dimethyl-1*H*-pyrrole-1-carboxylate **12** (0.789 g, 4.36 mmol) was diluted in dry THF (8 mL) and added drop wise over 15 minutes to the stirring solution. The mixture was then heated at reflux for a further 16 hours. The reaction was quenched with water (30 mL), transferred to a separating funnel and extracted with EtOAc (3 x 40 mL). The combined organic layer was washed with saturated aqueous Na₂CO₃ (2 x 50 mL) and brine (2 x 50 mL), dried over anhydrous MgSO₄ and concentrated *in vacuo*. The crude product was purified by silica-gel column chromatography using a petroleum spirit:acetone gradient of 100:0 to 80:20 to provide mixtures of the (*Z*) and (*E*)-isomers.

(*Z*)-Ethyl 3-(3,5-dimethyl-1*H*-pyrrol-2-yl)-2-(2-nitrophenyl)-acrylate ((*Z*)-3a**):** 42%, red crystalline solid; m.p. 124-126 °C; R_f = 0.50 (70:30 hexane:acetone); ¹H NMR (500 MHz, CDCl₃): δ 1.13 (t, 3H, *J* = 7.0 Hz), 2.17 (s, 3H), 2.35 (s, 3H), 4.12 (q, 2H, *J* = 7.0 Hz), 5.90 (s, 1H), 6.82 (s, 1H), 7.43 (m, 1H), 7.62 (t, 2H, *J* = 8.0 Hz), 8.02 (d, 1H, *J* = 8.0 Hz), 11.89 (br s, 1H); ¹³C NMR (125 MHz, CDCl₃): δ 13.7, 14.1, 29.9, 62.1, 111.5, 112.7, 124.1, 124.6, 127.8, 129.9, 131.5, 132.5, 133.5, 134.3, 137.5, 148.5, 163.8; IR (neat): ν(cm⁻¹) = 3275, 2354, 1684, 1577, 1569, 1544, 1518, 1367, 1335, 1319, 1262, 1196, 1153, 1026, 830, 789, 710 cm⁻¹; HRMS-ESI: *m/z* [M+H]⁺ calcd for C₁₇H₁₉N₂O₄: 315.1339, observed 315.1350.

(*E*)-Ethyl 3-(3,5-dimethyl-1*H*-pyrrol-2-yl)-2-(2-nitrophenyl)-acrylate ((*E*)-3b**):** 35%, red crystalline solid; m.p. 117-119 °C; R_f = 0.26 (70:30 hexane:acetone); ¹H NMR (500 MHz, CDCl₃): δ 1.19 (t, 3H, *J* = 7.0 Hz), 1.95 (s, 3H), 2.19 (s, 3H), 4.10 (dq, 1H, *J* = 4.0, 7.0 Hz), 4.23 (dq, 1H, *J* = 3.7, 7.0 Hz), 5.74 (s, 1H), 6.80 (br s, 1H), 7.49 (t, 1H, *J* = 7.5 Hz), 7.59 (t, 1H, *J* = 7.5 Hz), 7.67 (t, 1H, *J* = 7.5 Hz), 7.75 (s, 1H), 8.19 (d, 1H, *J* = 7.5 Hz); ¹³C NMR (125 MHz, CDCl₃): δ 11.3, 13.2, 14.1, 60.8, 110.7, 116.6, 123.4, 125.6, 127.2, 129.2, 130.1, 132.5, 133.3, 133.4, 136.7, 149.2, 166.6; IR (neat): ν(cm⁻¹) =

3447, 3421, 1700, 1618, 1607, 1564, 1518, 1338, 1180, 1147, 1093, 795 cm^{-1} ; HRMS-ESI: m/z $[\text{M}+\text{H}]^+$ calcd for $\text{C}_{17}\text{H}_{19}\text{N}_2\text{O}_4$: 315.1339, observed 315.1337.

(Z)-Methyl 3-(3,5-dimethyl-1H-pyrrol-2-yl)-2-(2-nitrophenyl)-acrylate ((Z)-4a): 36%, red crystalline solid; m.p. 66-68 °C; R_f = 0.47 (80:20 petroleum spirit:acetone); ^1H NMR (500 MHz, CDCl_3): δ 2.14 (s, 3H), 2.32 (s, 3H), 3.61 (s, 3H), 5.88 (s, 1H), 6.79 (s, 1H), 7.40 (d, 1H, J = 7.5 Hz), 7.41 (t, 1H, J = 7.5 Hz), 7.59 (t, 1H, J = 7.5 Hz), 8.00 (d, 1H, J = 7.5 Hz), 11.82 (br s, 1H); ^{13}C NMR (125 MHz, CDCl_3): δ 11.8, 13.9, 52.0, 111.6, 114.0, 124.5, 124.6, 128.0, 131.5, 134.4, 137.3, 148.5, 168.2; IR (neat): $\nu(\text{cm}^{-1})$ = 3455, 1691, 1603, 1555, 1522, 1430, 1343, 1222, 1190, 1172, 1149, 789, 718 cm^{-1} ; HRMS-ESI: m/z calcd for $\text{C}_{16}\text{H}_{17}\text{N}_2\text{O}_4$ $[\text{M} + \text{H}]^+$ 301.1183; observed 301.1185.

(E)-Methyl 3-(3,5-dimethyl-1H-pyrrol-2-yl)-2-(2-nitrophenyl)-acrylate ((E)-4b): 40%, red crystalline solid; m.p. 90-93 °C; R_f = 0.36 (80:20 petroleum spirit:acetone); ^1H NMR (500 MHz, CDCl_3): δ 1.95 (s, 3H), 2.20 (s, 3H), 3.70 (s, 3H), 5.74 (s, 1H), 6.74 (br s, 1H), 7.50 (d, 1H, J = 7.5 Hz), 7.61 (t, 1H, J = 7.5 Hz), 7.68 (t, 1H, J = 7.5 Hz), 7.75 (s, 1H), 8.20 (d, 1H, J = 7.5 Hz); ^{13}C NMR (126 MHz, CDCl_3): δ 11.6, 13.4, 52.3, 111.0, 116.3, 123.6, 125.5, 127.6, 129.4, 130.6, 132.7, 133.4, 133.8, 134.1, 149.4, 167.4; IR (neat): $\nu(\text{cm}^{-1})$ = 3293, 1689, 1570, 1544, 1518, 1432, 1365, 1334, 1317, 1263, 1195, 1180, 1151, 788, 709 cm^{-1} ; HRMS-ESI: m/z calcd for $\text{C}_{16}\text{H}_{17}\text{N}_2\text{O}_4$ $[\text{M} + \text{H}]^+$ 301.1183; observed 301.1182.

(Z)-Allyl 3-(3,5-dimethyl-1H-pyrrol-2-yl)-2-(2-nitrophenyl)-acrylate ((Z)-5a): 41%, deep red crystalline solid; m.p. 70-72 °C; R_f = 0.50 (80:20 petroleum spirit:acetone); ^1H NMR (500 MHz, CDCl_3): δ 2.17 (s, 3H), 2.35 (s, 3H), 4.56 (d, 2H, J = 5.5 Hz), 5.10 (dd, 1H, J = 1.5, 13.0 Hz), 5.13 (dd, 1H, J = 1.5, 6.5 Hz), 5.79 (m, 1H), 5.90 (s, 1H), 6.82 (s, 1H), 7.43 (d, 1H, J = 7.5 Hz), 7.44 (t, 1H, J =

7.5 Hz), 7.62 (t, 1H, $J = 7.5$ Hz), 8.04 (d, 1H, $J = 7.5$ Hz), 12.91 (br s, 1H); ^{13}C NMR (125 MHz, CDCl_3): δ 11.7, 13.8, 65.7, 111.6, 114.2, 118.1, 124.6, 124.7, 127.9, 131.5, 131.6, 132.9, 133.5, 134.4, 137.4, 148.9, 167.3; IR (neat): $\nu(\text{cm}^{-1}) = 3300, 2360, 1685, 1577, 1570, 1542, 1517, 1507, 1364, 1312, 1182, 1144, 966, 932, 858, 790 \text{ cm}^{-1}$; HRMS-ESI: m/z $[\text{M}+\text{H}]^+$ calcd for $\text{C}_{18}\text{H}_{19}\text{N}_2\text{O}_4$: 327.1339, observed 327.1342.

(E)-Allyl 3-(3,5-dimethyl-1H-pyrrol-2-yl)-2-(2-nitrophenyl)-acrylate ((E)-5b): 33%, red crystalline solid; m.p. 102-105 °C; $R_f = 0.40$ (80:20 petroleum spirit:acetone); ^1H NMR (500 MHz, CDCl_3): δ 1.95 (s, 3H), 2.19 (s, 3H), 4.59 (dd, 1H, $J = 5.5, 13.5$ Hz), 4.64 (dd, 1H, $J = 5.5, 13.5$ Hz), 5.15 (dd, 1H, $J = 1.5, 10.0$ Hz), 5.18 (dd, 1H, $J = 1.5, 18.5$ Hz), 5.74 (s, 1H), 5.85 (m, 1H), 6.75 (br s, 1H), 7.50 (d, 1H, $J = 8.0$ Hz), 7.60 (t, 1H, $J = 8.0$ Hz), 7.68 (t, 1H, $J = 8.0$ Hz), 7.77 (s, 1H), 8.19 (d, 1H, $J = 8.0$ Hz); ^{13}C NMR (125 MHz, CDCl_3): δ 11.5, 13.4, 65.6, 111.0, 116.3, 117.7, 123.6, 125.4, 127.6, 129.5, 130.6, 132.5, 133.3, 133.7, 134.1, 149.4, 166.5; IR (neat): $\nu(\text{cm}^{-1}) = 3455, 1687, 1610, 1557, 1524, 1343, 1257, 1232, 1068, 869, 733 \text{ cm}^{-1}$; HRMS-ESI: m/z $[\text{M}+\text{H}]^+$ calcd for $\text{C}_{17}\text{H}_{19}\text{N}_2\text{O}_4$ 327.1339, observed 327.1333.

(Z)-3-(3,5-Dimethyl-1H-pyrrol-2-yl)-N-ethyl-2-(2-nitrophenyl)-acrylamide ((Z)-6a): 21%, red crystalline solid; m.p. 96-99 °C; $R_f = 0.17$ (80:20 petroleum spirit:acetone); ^1H NMR (500 MHz, CDCl_3): δ 1.07 (t, 3H, $J = 7.0$ Hz), 2.09 (s, 3H), 2.31 (s, 3H), 3.31 (q, 2H, $J = 7.0$ Hz), 5.18 (br s, 1H), 5.82 (s, 1H), 6.46 (s, 1H), 7.52 (m, 2H), 7.65 (t, 1H, $J = 8.0$ Hz), 7.98 (d, 1H, $J = 8.0$ Hz), 12.21 (br s, 1H); ^{13}C NMR (125 MHz, CDCl_3): δ 11.3, 13.5, 14.6, 34.8, 110.6, 116.4, 124.0, 124.7, 128.0, 128.7, 128.8, 132.9, 133.3, 133.4, 136.3, 149.5, 167.5; IR (neat): $\nu(\text{cm}^{-1}) = 3408, 1639, 1576, 1569, 1517, 1457, 1350, 1224 \text{ cm}^{-1}$; HRMS-ESI: m/z $[\text{M}+\text{H}]^+$ calcd for $\text{C}_{17}\text{H}_{20}\text{N}_3\text{O}_3$ 314.1499, observed 314.1497.

(Z)-3-(3,5-Dimethyl-1H-pyrrol-2-yl)-2-(2-nitrophenyl)-N-phenylacrylamide ((Z)-7a): 22%, red crystalline solid; m.p. 177-179 °C; $R_f = 0.36$ (80:20 petroleum spirit:acetone); $^1\text{H NMR}$ (500 MHz, CDCl_3): δ 2.12 (s, 3H), 2.32 (s, 3H), 5.86 (s, 1H), 6.56 (s, 1H), 6.87 (br s, 1H), 7.12 (t, 1H, $J = 7.5$ Hz), 7.32 (t, 2H, $J = 7.5$ Hz), 7.37 (t, 2H, $J = 7.5$ Hz), 7.56 (t, 1H, $J = 8.0$ Hz), 7.60 (d, 1H, $J = 8.0$ Hz), 7.71 (t, 1H, $J = 8.0$ Hz), 8.03 (d, 1H, $J = 8.0$ Hz), 12.00 (br s, 1H); $^{13}\text{C NMR}$ (125 MHz, CDCl_3): δ 11.4, 13.6, 111.1, 115.6, 121.4, 124.1, 124.9, 129.0, 129.1, 130.1, 133.5, 133.5, 133.8, 135.8, 137.4, 149.7, 166.2; IR (neat): $\nu(\text{cm}^{-1}) = 3400, 1650, 1595, 1592, 1518, 1498, 1436, 1362, 1352, 1318, 1229, 1188, 1151, 1004, 802, 790, 772, 759, 739, 718$ cm^{-1} ; HRMS-ESI: m/z $[\text{M}+\text{H}]^+$ calcd for $\text{C}_{21}\text{H}_{20}\text{N}_3\text{O}_3$ 362.1499, observed 362.1521.

(E)-3-(3,5-Dimethyl-1H-pyrrol-2-yl)-2-(2-nitrophenyl)-N-phenylacrylamide ((E)-7b): <5%, red amorphous solid (impure, not tested in angiogenesis inhibition assay); $^1\text{H NMR}$ (500 MHz, CDCl_3): δ 1.92 (s, 3H), 2.13 (s, 3H), 5.70 (s, 1H), 6.47 (br s, 1H), 7.04 (t, 1H, $J = 7$ Hz), 7.14 (br s, 1H), 7.24 (t, 2H, $J = 7.5$ Hz), 7.43 (d, 2H, $J = 8.0$ Hz), 7.57 (d, 1H, $J = 7.5$ Hz), 7.68 (s, 1H), 7.75 (t, 1H, $J = 7.5$ Hz), 7.66 (m, 1H), 8.13 (d, 1H, $J = 8.0$ Hz); $^{13}\text{C NMR}$ (125 MHz, CDCl_3): δ 11.2, 13.1, 110.6, 118.9, 120.4, 123.3, 124.1, 125.1, 125.4, 128.7, 129.6, 130.3, 131.5, 133.5, 133.8, 134.3, 138.0, 149.4, 165.0. HRMS-ESI: m/z $[\text{M}+\text{H}]^+$ calcd for $\text{C}_{21}\text{H}_{20}\text{N}_3\text{O}_3$ 362.1499, observed 362.1503.

(Z)-N-benzyl-3-(3,5-dimethyl-1H-pyrrol-2-yl)-2-(2-nitrophenyl)acrylamide ((Z)-8a): 16%, red crystalline solid; m.p. 140-142 °C; $R_f = 0.36$ (80:20 petroleum spirit:acetone); $^1\text{H NMR}$ (500 MHz, CDCl_3): δ 2.09 (s, 3H), 2.31 (s, 3H), 4.50 (d, 2H, $J = 6$ Hz), 5.50 (br s, 1H), 5.83 (s, 1H), 6.48 (s, 1H), 7.20 (d, 2H, $J = 8.0$ Hz), 7.22 (m, 1H, $J = 7.0$ Hz), 7.28 (t, 2H, $J = 7.5$ Hz), 7.47 (m, 1H, $J = 8.0$ Hz), 7.49 (m, 1H, $J = 6.5$ Hz), 7.61 (t, 1H, $J = 7.5$ Hz), 7.94 (d, 1H, $J = 8.5$ Hz), 12.21 (br s, 1H); $^{13}\text{C NMR}$ (125 MHz, CDCl_3): δ 11.3, 13.7, 43.9, 110.7, 115.8, 124.0, 124.7, 127.3, 127.3, 128.3, 128.6, 128.9,

129.2, 133.1, 133.3, 133.4, 136.0, 138.0, 167.6; IR (neat): $\nu(\text{cm}^{-1}) = 3435, 1643, 1570, 1543, 1507, 1453, 1362, 1341, 1316, 1237, 1217, 1150, 786, 728, 709 \text{ cm}^{-1}$; HRMS-ESI: m/z $[\text{M}+\text{H}]^+$ calcd for $\text{C}_{22}\text{H}_{22}\text{N}_3\text{O}_3$ 376.1656, observed 376.1668.

(E)-N-benzyl-3-(3,5-dimethyl-1H-pyrrol-2-yl)-2-(2-nitrophenyl)acrylamide ((E)-8b): <5%, red amorphous solid (impure, not tested in angiogenesis inhibition assay); ^1H NMR (500 MHz, CDCl_3): δ 2.09 (s, 3H), 2.31 (s, 3H), 4.50 (d, 2H, $J = 6$ Hz), 5.50 (br s, 1H), 5.83 (s, 1H), 6.48 (s, 1H), 7.20 (d, 2H, $J = 8.0$ Hz), 7.22 (m, 1H, $J = 7.0$ Hz), 7.28 (t, 2H, $J = 7.5$ Hz), 7.47 (m, 1H, $J = 8.0$ Hz), 7.49 (m, 1H, $J = 6.5$ Hz), 7.61 (t, 1H, $J = 7.5$ Hz), 7.94 (d, 1H, $J = 8.5$ Hz). Note: due to impurities the chemical shift of the pyrrolic NH signal could not be assigned unambiguously; ^{13}C NMR (125 MHz, CDCl_3): δ 11.3, 13.6, 43.9, 110.7, 115.8, 124.0, 124.7, 127.3, 127.3, 128.4, 128.6, 128.9, 129.3, 133.088, 133.3, 133.4, 136.0, 137.974, 167.6; HRMS-ESI: m/z $[\text{M}+\text{H}]^+$ calcd for $\text{C}_{22}\text{H}_{22}\text{N}_3\text{O}_3$ 376.1656, observed 376.1675.

General method for condensation reactions to produce alkenes (Z)-9a, (E)-9b and (Z)-10a, (E)-10b: Method b: Dry *N,N*-diisopropylamine (4.60 mmol) was dissolved in dry THF (7 mL) under Ar in a 3-neck 100 mL round bottom flask. The flask was cooled to -78 °C and *n*-butyllithium (4.60 mmol) was added and stirred for 20 minutes. Ethyl-2-phenylacetate **19** or ethyl-2-(2-chlorophenyl)-acetate **20** (4.28 mmol) was then added dropwise as a solution in dry THF (1 mL) and the reaction was stirred for a further 30 minutes. Methyl 2-formyl-3,5-dimethyl-1*H*-pyrrole-1-carboxylate **12** (0.757 g, 4.18 mmol) was subsequently added dropwise as a solution in dry THF (1 mL) and the reaction stirred for a further 30 min, with monitoring by TLC (75:25 petroleum spirit:EtOAc). The reaction was quenched with saturated aqueous NH_4Cl (30 mL) and the solvent removed *in vacuo*. EtOAc (30 mL) was added to the residue and the organic layer was washed with saturated aqueous NH_4Cl (3 x 25 mL), saturated

aqueous Na₂CO₃ (2 x 25 mL) and brine (30 mL), before being dried over anhydrous MgSO₄ and concentrated *in vacuo*. The crude product was purified by silica-gel chromatography column with a gradient from 100:0 to 70:30 petroleum spirit:EtOAc to provide mixtures of the (*Z*) and (*E*)-isomers.

(E)-Ethyl 3-(3,5-dimethyl-1H-pyrrol-2-yl)-2-phenylacrylate ((E)-9b): 32%, yellow crystalline solid; m.p. 62-64 °C; R_f = 0.43 (75:25 petroleum spirit:EtOAc); ¹H NMR (500 MHz, CDCl₃): δ 1.26 (t, 3H, *J* = 7.0 Hz), 1.91 (s, 3H), 2.19 (s, 3H), 4.22 (q, 2H, *J* = 7.0 Hz), 5.69 (s, 1H), 6.84 (br s, 1H), 7.32 (d, 2H, *J* = 7.0 Hz), 7.43 (t, 1H, *J* = 7.0 Hz), 7.46 (t, 2H, *J* = 7.0 Hz), 7.75 (s, 1H); ¹³C NMR (125 MHz, CDCl₃): δ 11.2, 13.1, 14.4, 60.5, 110.0, 120.5, 124.1, 127.4, 127.9, 128.8, 129.0, 130.2, 132.9, 137.3, 169.2; IR (neat): ν (cm⁻¹) = 3442, 1697, 1607, 1560, 1497, 1227 cm⁻¹; HRMS-ESI: *m/z* [M+H]⁺ calcd for C₁₇H₂₀NO₂ 270.1489, observed 270.1488.

(Z)-Ethyl 3-(3,5-dimethyl-1H-pyrrol-2-yl)-2-(2-chlorophenyl)-acrylate ((Z)-10a): 5%, yellow crystalline solid; m.p. 124-126 °C; R_f = 0.71 (70:30 petroleum spirit:EtOAc); ¹H NMR (500 MHz, CDCl₃): δ 1.20 (t, 3H, *J* = 7.0 Hz), 2.14 (s, 3H), 2.33 (s, 3H), 4.20 (q, 2H, *J* = 7.0 Hz), 5.87 (s, 1H), 6.72 (s, 1H), 7.25 (m, 2H), 7.31 (d, 1H, *J* = 7.0 Hz), 7.38 (d, 1H, *J* = 7.0 Hz), 11.80 (br s, 1H); ¹³C NMR (125 MHz, CDCl₃): δ 11.6, 13.8, 14.3, 61.0, 111.3, 116.1, 124.4, 126.9, 128.3, 129.2, 130.6, 131.8, 132.2, 133.6, 135.1, 141.2, 168.9; IR (neat): ν (cm⁻¹) = 3273, 1680, 1576, 1545, 1465, 1188, 736 cm⁻¹; HRMS-ESI: *m/z* [M+H]⁺ calcd for C₁₇H₁₉NO₂Cl 304.1099, observed 304.1099.

(E)-Ethyl 3-(3,5-dimethyl-1H-pyrrol-2-yl)-2-(2-chlorophenyl)-acrylate ((E)-10b): 41%, yellow amorphous solid; m.p. 70-74 °C; R_f = 0.39 (75:25 petroleum spirit:EtOAc); ¹H NMR (CDCl₃, 500 MHz): δ 1.24 (t, 3H, *J* = 7.0 Hz), 1.93 (s, 3H), 2.20 (s, 3H), 4.18 (q, 1H, *J* = 7.0 Hz), 4.25 (q, 2H, *J* = 7.0 Hz), 5.74 (s, 1H), 6.75 (br s, 1H), 7.3 (m, 3H), 7.54 (d, 1H, *J* = 8 Hz), 7.78 (s, 1H); ¹³C NMR (125

MHz, CDCl₃): δ 11.2, 13.1, 14.3, 60.6, 110.3, 117.7, 123.9, 127.3, 128.1, 129.5, 129.5, 130.1, 131.9, 133.5, 135.1, 136.3, 167.4; IR (neat): $\nu(\text{cm}^{-1}) = 3447, 1697, 1603, 1558, 1473, 1226, 745 \text{ cm}^{-1}$; HRMS-ESI: m/z [M+H]⁺ calcd for C₁₇H₁₉NO₂Cl 304.1099, observed 304.1092.

5.2. X-Ray Crystallography

Crystal data Compound (*Z*)-**5a**. C₁₈H₁₈N₂O₄, $M=326.35$, $T=200 \text{ K}$, monoclinic, space group $P2_1/c$, $Z=4$, $a=12.5669(4)$, $b=7.9086(3)$, $c=17.6200(4) \text{ \AA}$, $\beta=103.730(2)^\circ$, $V=1701.15(6) \text{ \AA}^3$, $D_x=1.274 \text{ g/cm}^3$, 32664 reflections measured ($2\theta=5\text{--}55^\circ$) merged to 3903 unique data, $R=0.053$ [for 2656 data with $I>2\sigma(I)$], $R_w=0.147$ [all data], $S=0.95$. Compound (*E*)-**5b**. C₁₈H₁₈N₂O₄, $M=326.35$, $T=298(2) \text{ K}$, triclinic, space group $P-1$, $Z=2$, $a=8.4326(4)$, $b=10.2147(4)$, $c=11.0598(6) \text{ \AA}$, $\alpha=72.485(3)^\circ$, $\beta=76.605(2)^\circ$, $\gamma=71.312(3)^\circ$, $V=850.89(7) \text{ \AA}^3$, $D_x=1.274 \text{ g/cm}^3$, 7615 reflections measured ($2\theta=4\text{--}54.2^\circ$) merged to 3674 unique data, $R=0.064$ [for 2849 data with $I>2\sigma(I)$], $R_w=0.187$ [all data], $S=0.99$.

Structure determination Images were measured on Nonius KappaCCD diffractometers (Mo $K\alpha$ radiation, graphite monochromator, $\lambda=0.71073 \text{ \AA}$) and data were extracted using the DENZO package.^[26] For (*Z*)-**5a**, structure solution was by direct methods (SIR92)^[27] and the structure was refined using the CRYSTALS program package.^[28] For (*E*)-**5b**, structure solution was by direct methods (SIR97)^[29] and the structure was refined using the SHELXL-97 program package.^[30] Atomic coordinates, bond lengths and angles and displacement parameters have been deposited at the Cambridge Crystallographic Data Centre (CCDC accession numbers 905343 and 905344, respectively). These data can be obtained free-of-charge via www.ccdc.cam.ac.uk/data_request/cif, by emailing data_request@ccdc.cam.ac.uk, or by contacting The Cambridge Crystallographic Data Centre, 12 Union Road, Cambridge CB2 1EZ, UK; fax: +44 1223 336033.

5.3. Angiogenesis Inhibition Assay

Compounds were tested for angiogenesis inhibition in 48-well culture plates using the previously reported *in vitro* assay with some modifications.^[23] Briefly, the thoracic aortas from female Fischer 344 rats were excised and the 2.5cm long vessels placed in HBSS media containing 2.5 µg/mL amphotericin B and cross-sectioned at 1mm intervals. In the angiogenesis assay 15 µL of bovine thrombin (50 NIH unit/mL in 0.15 M NaCl) was added to each well, followed by 0.5 mL/well of 3 mg/mL bovine fibrinogen in Medium 199. The thrombin and fibrinogen were mixed rapidly and one vessel section was quickly placed in the center of the well before clot formation. Fibrin gel formation usually occurred within 0.5 min leaving the vessel fragment suspended in the gel. Upon gel formation, 0.5 mL/well of Medium 199 supplemented with 20% FCS, 0.1% ε-amino caproic acid, L-glutamine, and antibiotics (gentamicin sulphate and amphotericin B) and test compound were added. Six replicate cultures were examined for each concentration of test compound. Vessels were cultured at 37 °C in 5% CO₂ in a humidified environment for 7 days, with the medium being changed on Day 4. On Day 5 the percentage of the field of view occupied by vessel outgrowths (FOV occupancy %) was used as a quantitative measure of angiogenesis (inhibition) relative to control (no compound added).

Acknowledgments

P. Sudta and S. Suksamrarn acknowledge financial support from the Thailand Research Fund through the Royal Golden Jubilee PhD Program. S. Prapbai and P. Kongsaree thank the National Research University Project through Mahidol University for financial support. M. Kelso acknowledges partial financial support from the University of Wollongong URC Small Grants Scheme. A. Bezos and C. R. Parish acknowledge support from an Australian National Health and Medical Research Council (NHMRC) Program Grant.

Supplementary data

Supplementary data associated with this article can be found, in the online version, at <http://XXXXXX>.

These data include ^1H NMR spectra for (*Z*)-**3a** and (*E*)-**3b** and angiogenesis inhibition assay statistics.

References

- (1) Hanahan, D.; Folkman, J. *Cell* **1996**, 86, 353.
- (2) Carmeliet, P. *Nat. Med.* **2003**, 9, 653.
- (3) Zetter, B. R. *Annu. Rev. Med.* **1998**, 49, 407.
- (4) Shojaei, F. *Cancer Lett.* **2012**, 320, 130.
- (5) Hurwitz, H.; Fehrenbacher, L.; Novotny, W.; Cartwright, T.; Hainsworth, J.; Heim, W.; Berlin, J.; Baron, A.; Griffing, S.; Holmgren, E.; Ferrara, N.; Fyfe, G.; Rogers, B.; Ross, R.; Kabbinavar, F. *New Engl. J. Med.* **2004**, 350, 2335.
- (6) Sandler, A.; Gray, R.; Perry, M. C.; Brahmer, J.; Schiller, J. H.; Dowlati, A.; Lilienbaum, R.; Johnson, D. H. *New Engl. J. Med.* **2006**, 355, 2542.
- (7) Miller, K.; Wang, M.; Gralow, J.; Dickler, M.; Cobleigh, M.; Perez, E. A.; Shenkier, T.; Cella, D.; Davidson, N. E. *New Engl. J. Med.* **2007**, 357, 2666.
- (8) Holash, J.; Davis, S.; Papadopoulos, N.; Croll, S. D.; Ho, L.; Russell, M.; Boland, P.; Leidich, R.; Hylton, D.; Burova, E.; Ioffe, E.; Huang, T.; Radziejewski, C.; Bailey, K.; Fandl, J. P.; Daly, T.; Wiegand, S. J.; Yancopoulos, G. D.; Rudge, J. S. *P. Natl. Acad. Sci. USA.* **2002**, 99, 11393.
- (9) O'Farrell, A-M.; Abrams, T. J.; Yuen, H. A.; Ngai, T. J.; Louie, S. G.; Yee, K. W. H.; Wong, L. M.; Hong, W.; Lee, L. B.; Town, A.; Smolich, B. D.; Manning, W. C.; Murray, L. J.; Heinrich, M. C.; Cherrington, J. M. *Blood* **2003**, 101, 3597.
- (10) van der Graaf, W. T. A.; Blay, J-Y.; Chawla, S. P.; Kim, D-W.; Bui-Nguyen, B.; Casali, P. G.; Schöffski, P.; Aglietta, M.; Staddon, A. P.; Beppu, Y.; Le Cesne, A.; Gelderblom, H.; Judson, I.

- R.; Araki, N.; Ouali, M.; Marraud, S.; Hodge, R.; Dewji, M. R.; Coens, C.; Demetri, G. D.; Fletcher, C. D.; Dei Tos, A. P.; Hohenberger, P. *Lancet* **2012**, 379, 1879.
- (11) Kupsch, P.; Henning, B. F.; Passarge, K.; Richly, H.; Wiesemann, K.; Hilger, R. A.; Scheulen, M. E.; Christensen, O.; Brendel, E.; Schwartz, B.; Hofstra, E.; Voigtmann, R.; Seeber, S.; Strumberg, D. *Clin. Colorectal Canc.* **2005**, 5, 188.
- (12) Wu, X.; Jin, Y.; Cui, I. H.; Xu, Z.; Zhang, Y.; Zhang, X.; Tang, C.; Gong, Y.; Chen, J. *Anti-Cancer Drug* **2012**, 23, 731.
- (13) Wood, L. *Expert Opin. Pharmacother.* **2012**, 13, 1323.
- (14) Koshenkov, V. P.; Rodgers, S. E. *Curr. Opin. Oncol.* **2012**, 24, 414.
- (15) Zhou, C.; Zhang, J.; Zheng, Y.; Zhu, Z. *Int. J. Cancer* **2012**, 131, 1013.
- (16) Roskoski Jr., R. *Biochem. Bioph. Res. Co.* **2007**, 356, 323.
- (17) Prakash, C. R.; Raja, S. *Mini-Rev. Med. Chem.* **2012**, 12, 98.
- (18) Sun, L.; Liang, C.; Shirazian, S.; Zhou, Y.; Miller, T.; Cui, J.; Fukuda, J. Y.; Chu, J-Y.; Nematalla, A.; Wang, X.; Chen, H.; Sistla, A.; Luu, T. C.; Tang, F.; Wei, J.; Tang, C. *J. Med. Chem.* **2003**, 46, 1116.
- (19) Abell, A. D.; Nabbs, B. K.; Battersby, A. R. *J. Am. Chem. Soc.* **1998**, 120, 1741.
- (20) Schauder, J-R.; Jendrzejewski, S.; Abell, A.; Hart, G. J.; Battersby, A. R. *J. Chem. Soc. Chem. Commun.* **1987**, 436
- (21) Arunan, E.; Desiraju, G. R.; Klein, R. A.; Sadlej, J.; Scheiner, S.; Alkorta, I.; Clary, D. C.; Crabtree, R. H.; Dannenberg, J. J.; Hobza, P.; Kjaergaard, H. G.; Legon, A. C.; Mennucci, B.; Nesbitt, D. J. *Pure Appl. Chem.* **2011**, 83, 1637.
- (22) Sun, L.; Tran, N.; Tang, F.; App, H.; Hirth, P.; McMahon, G.; Tang, C. *J. Med. Chem.* **1998**, 41, 2588.
- (23) Brown, K. J.; Maynes, S. F.; Bezos, A.; Maguire, D. J.; Ford, M. D.; Parish, C. R. *Lab. Invest.* **1996**, 75, 539.

- (24) Parish, C. R.; Freeman, C.; Brown, K. J.; Francis, D. J.; Cowden, W. B. *Cancer Res.* **1999**, *59*, 3433.
- (25) <http://www.cancer.gov/clinicaltrials/search/view?cdrid=706994&version=HealthProfessional&protocolsearchid=7230273> (Accessed Oct 22, 2012).
- (26) Z. Otwinowski. Minor, Processing of X-ray diffraction data collected in oscillation mode. In *Methods in Enzymology*, C. W. Carter Jr., R. M. Sweet, Eds.; Macromolecular Crystallography, Part A; Academic: New York, NY, **1997**, 276, 307.
- (27) Altomare, A.; Cascarano, G.; Giacovazzo, C.; Guagliardi, A.; Burla, M. C.; Polidori, G.; Camalli, M. *J. Appl. Crystallogr.*, **1994**, *27*, 435.
- (28) Betteridge, P. W.; Carruthers, J. R.; Cooper, R. I.; Prout, K.; Watkin, D. J. *J. Appl. Crystallogr.* **2003**, *36*, 1487.
- (29) Altomare, A.; Burla, M. C.; Camalli, M.; Cascarano, G. L.; Giacovazzo, C.; Guagliardi, A.; Moliterni, A. G. G.; Polidori, G.; Spagna, R. *J. Appl. Crystallogr.*, **1999**, *32*, 115.
- (30) Sheldrick, G. M. *Acta Crystallogr., Section A*, **2008**, *64*, 112.